

# LpMab-19 Recognizes Sialylated O-Glycan on Thr76 of Human Podoplanin

Satoshi Ogasawara, Mika K. Kaneko, and Yukinari Kato

Human podoplanin (hPDPN) is expressed in lymphatic vessels, pulmonary type-I alveolar cells, and renal glomerulus. The hPDPN/C-type lectin-like receptor-2 (CLEC-2) interaction is involved in platelet aggregation and cancer metastasis. High expression of hPDPN in cancer cells or cancer-associated fibroblasts (CAFs) leads to a poor prognosis for cancer patients. In our previous research, we reported on several anti-hPDPN monoclonal antibodies (mAbs), including LpMab-2, LpMab-3, LpMab-7, LpMab-9, LpMab-12, LpMab-13, and LpMab-17 of mouse IgG<sub>1</sub> subclass, which were produced using CasMab technology. Here we produced a novel anti-hPDPN mAb LpMab-19 of mouse IgG<sub>2b</sub> subclass. Flow cytometry revealed that the epitope of LpMab-19 includes O-glycan, which is attached to Thr76 of hPDPN. We further identified the minimum epitope of LpMab-19 as Thr76–Arg79 of hPDPN. Immunohistochemistry revealed that LpMab-19 is useful for detecting not only normal cells, including lymphatic vessels, but also glioblastoma and oral squamous cell carcinoma cells. LpMab-19 could be useful for investigating the physiological function of O-glycosylated hPDPN.

**Keywords:** podoplanin, PDPN, CasMab, glycopeptide, monoclonal antibody

## Introduction

**T**O DETERMINE THE PHYSIOLOGICAL function of membrane proteins in normal tissues and cancers, it is necessary to have highly sensitive and specific monoclonal antibodies (mAbs). Human podoplanin (hPDPN), known as a platelet aggregation-inducing (PLAG) factor (gp44/Aggrus), is involved in cancer metastasis.<sup>(1–10)</sup> We have produced many anti-hPDPN mAbs,<sup>(11–21)</sup> including NZ-1, which was produced by immunizing rats with the synthetic peptide (hpp3851) of hPDPN, and it has high specificity, sensitivity, and binding affinity for hPDPN.<sup>(21–23)</sup> The high binding affinity of NZ-1 has also been confirmed by other studies.<sup>(24,25)</sup> NZ-1 was highly internalized into glioma cell lines and also well accumulated into tumors *in vivo*; therefore, NZ-1 is a suitable candidate for therapy against malignant gliomas.<sup>(23,26)</sup> NZ-1 has antibody-dependent cellular cytotoxicity and complement-dependent cytotoxicity against hPDPN-expressing tumor cells.<sup>(27)</sup> Furthermore, NZ-1 inhibited the tumor cell-induced platelet aggregation and tumor metastasis by its neutralizing activity.<sup>(28)</sup> NZ-1 possesses good applications in many experiments, such as western blot, flow cytometry, immunohistochemical analysis, and immunoprecipitation.

We recently established the CasMab technology, which produces cancer-specific mAbs, although one protein in the cancer and normal cells has the same amino acid sequence.<sup>(11)</sup> We used LN229/hPDPN cells, not purified recombinant proteins, for immunization to develop novel anti-hPDPN mAbs.

Although we have produced many anti-hPDPN mAbs using CasMab technology,<sup>(11–17,19,20)</sup> almost all mAbs, including LpMab-2, LpMab-3, LpMab-7, LpMab-9, LpMab-12, LpMab-13, and LpMab-17, were determined to belong to the IgG<sub>1</sub> subclass. Only the clone LpMab-10 was classified as IgG<sub>3</sub> subclass; however, mouse IgG<sub>3</sub> subclass is often aggregated.<sup>(29)</sup> Furthermore, almost all anti-hPDPN mAbs react with PLAG domains (PLAG1–PLAG3) of hPDPN.<sup>(21,22,30–33)</sup> A novel PLAG domain of hPDPN was recently reported as PLAG4<sub>(81–EDLPT-85)</sub>, and anti-PLAG4 mAbs were produced.<sup>(34)</sup> We need to produce further anti-hPDPN mAbs, which target different epitopes of hPDPN, to fully understand the pathophysiological function of hPDPN.

Here we produced a novel anti-hPDPN mAb, LpMab-19 (mouse IgG<sub>2b</sub>, kappa), the epitope of which is a O-glycosylated glycopeptide of hPDPN.

## Materials and Methods

### Cell lines

LN229, HEK-293T, Chinese hamster ovary (CHO)-K1, and P3U1 were obtained from the American Type Culture Collection (ATCC, Manassas, VA). LN319 was donated by Prof. Kazuhiko Mishima (Saitama Medical University, Saitama, Japan).<sup>(35)</sup> CHO-S was purchased from Thermo Fisher Scientific, Inc. (Waltham, MA). LN229 was previously transfected with hPDPN plasmids (LN229/hPDPN) using Lipofectamine 2000 (Thermo Fisher Scientific, Inc.) according

to the manufacturer's instructions.<sup>(11)</sup> The HEK-293T/hPDPN-knockout (KO) cell line (PDIS-2) and the LN319/hPDPN-KO cell line (PDIS-6) were generated by transfection using CRISPR/Cas plasmids (Target ID: HS0000333287) that target PDPN (Sigma-Aldrich, St. Louis, MO). PDIS-2 and PDIS-6 cells were screened using the NZ-1 mAb.<sup>(12,15,18–20)</sup>

CHO-K1 and P3U1 were cultured in RPMI 1640 medium, including L-glutamine (Nacalai Tesque, Inc., Kyoto, Japan) supplemented with 10% heat-inactivated fetal bovine serum (FBS; Thermo Fisher Scientific, Inc.). CHO-S was cultured using CHO-S-SFM II (Thermo Fisher Scientific, Inc.). LN229, LN229/hPDPN, LN319, HEK-293T, PDIS-2, and PDIS-6 were cultured in Dulbecco's modified Eagle's medium, including L-glutamine (Nacalai Tesque, Inc.), supplemented with 10% heat-inactivated FBS at 37°C in a humidified atmosphere of 5% CO<sub>2</sub> and 95% air. Antibiotics, including 100 units/mL of penicillin, 100 µg/mL of streptomycin, and 25 µg/mL of amphotericin B (Nacalai Tesque, Inc.), were added to all media.

#### Production of deletion mutants

The amplified *hPDPN* complementary DNA (cDNA) was subcloned into a pCAG-Ble(Zeo) vector (Wako Pure Chemical Industries Ltd. [Osaka, Japan]) with an MAP tag, which was detected by PMab-1<sup>(36,37)</sup> and added at the N-terminus using In-Fusion HD cloning kit (Clontech Laboratories Inc., Mountain View, CA). Deletion mutants of *hPDPN* were produced using several primers. Sense primers used were as follows: AGAAGACAAAAAGCTTGCCAGCACAGGCC AGCC for dN23, AGAAGACAAAAAGCTTGAAGGCG GCGTTGCCAT for dN37, AGAAGACAAAAAGCTTGCC GAAGATGATGTGGTG for dN46, AGAAGACAAAA GCTTACCAGCGAAGACCGCTA for dN55, AGAAGAC AAAAAGCTTACAACCTTGGTGCAACA for dN64, AG AAGACAAAAAGCTTGTAACAGGCATTTCGCATC for dN75, AGAAGACAAAAAGCTTACTTCAGAAAGCACA GTCC for dN85, AGAAGACAAAAAGCTTCAAAGTCC AAGCGCCAC for dN95, AGAAGACAAAAAGCTTGCC ACCAGTCACTCCAC for dN105.

The following antisense primer was used: TCTAGAG TCGCGGCCGCTTACTTGTCTGCATCGT.

CHO-K1 cells were transfected with the plasmids using a Lipofectamin LTX (Thermo Fisher Scientific, Inc.). Deletion mutants were cultured in RPMI 1640 medium including L-glutamine supplemented with heat-inactivated FBS. Stable transfectants of CHO-K1/ssMAP-hPDPNΔN mutants were selected by cultivating the transfectants in a medium containing 0.5 mg/mL of zeocin (InvivoGen, Inc., San Diego, CA).

#### Production of point mutants

The amplified *hPDPN* cDNA was subcloned into a pcDNA3 vector (Thermo Fisher Scientific, Inc.), and a FLAG epitope tag was added at the C-terminus. Amino acids in *hPDPN* were substituted with alanine or glycine using a QuikChange Lightning site-directed mutagenesis kit (Agilent Technologies, Inc., Santa Clara, CA) with oligonucleotides containing the desired mutations. CHO-S or CHO-K1 cells were transfected with the plasmids using a Gene Pulser Xcell electroporation system (Bio-Rad Laboratories, Inc., Berke-

ley, CA). Point mutants of CHO-K1 and CHO-S were cultured in RPMI 1640 medium including L-glutamine supplemented with heat-inactivated FBS and CHO-S-SFM II, respectively.

#### Hybridoma production

Four-week-old female BALB/c mice (CLEA Japan, Tokyo, Japan) were immunized by intraperitoneal (i.p.) injection of  $1 \times 10^8$  LN229/hPDPN cells together with Inject Alum (Thermo Fisher Scientific, Inc.).<sup>(11)</sup> After several additional immunizations, a booster i.p. injection was given 2 days before mice were euthanized by cervical dislocation, and spleen cells were harvested. The spleen cells were fused with P3U1 cells using PEG1500 (Roche Diagnostics, Indianapolis, IN). Hybridomas were grown in RPMI 1640 medium including L-glutamine with hypoxanthine, aminopterin, and thymidine selection medium supplement (Thermo Fisher Scientific, Inc.). Culture supernatants were screened using enzyme-linked immunosorbent assay (ELISA) for binding to recombinant hPDPN purified from LN229/hPDPN cells. Proteins were immobilized on Nunc Maxisorp 96-well immunoplates (Thermo Fisher Scientific, Inc.) at 1 µg/mL for 30 minutes. After blocking with 1% bovine serum albumin (BSA) in 0.05% Tween20/phosphate-buffered saline (PBS; Nacalai Tesque, Inc.), the plates were incubated with culture supernatant followed by 1:2000 diluted peroxidase-conjugated antimouse IgG (Agilent Technologies, Inc.). The enzymatic reaction was produced with a 1-Step Ultra TMB-ELISA (Thermo Fisher Scientific, Inc.). Optical density was measured at 655 nm using an iMark microplate reader (Bio-Rad Laboratories, Inc.).

#### Flow cytometry

Cell lines were harvested by brief exposure to 0.25% trypsin/1 mM EDTA (Nacalai Tesque, Inc.). After washing with 0.1% BSA in PBS, cells were treated with primary mAbs for 30 minutes at 4°C, followed by treatment with Oregon Green 488 goat antimouse IgG or antirat IgG (Thermo Fisher Scientific, Inc.). Fluorescence data were collected using a Cell Analyzer EC800 (Sony Corp., Tokyo, Japan).

#### Immunohistochemical analyses

The use of human cancer tissues was reviewed and approved by Sendai Medical Center Review Board.<sup>(19)</sup> Written informed consent was obtained for the human cancer tissue samples used in this study. Four-micrometer-thick histologic sections were deparaffinized in xylene and rehydrated. After antigen retrieval procedure (autoclave using citrate buffer, pH 6.0; Agilent Technologies, Inc.), sections were incubated with 1 µg/mL of LpMab-19 for 1 hour at room temperature followed by treatment with Envision+ kit (Agilent Technologies, Inc.) for 30 minutes. Color was developed using 3,3'-diaminobenzidine tetrahydrochloride (Agilent Technologies, Inc.) for 5 minutes, and then the sections were counterstained with hematoxylin (Wako Pure Chemical Industries Ltd.).

## Results and Discussion

The expression of hPDPN has been reported in many cancers, such as oral cancer, lung cancer, esophageal cancer, malignant mesothelioma, malignant glioma, testicular tumor,

bladder cancer, and osteosarcoma.<sup>(8,21,23,26,38–46)</sup> hPDPN is a PLAG factor, which is involved in cancer metastasis.<sup>(8–10)</sup> hPDPN-expressing cancer-associated fibroblasts are associated with poor prognosis of several cancers.<sup>(47–52)</sup> We previously identified C-type lectin-like receptor-2 (CLEC-2) as an endogenous receptor of hPDPN,<sup>(28,53)</sup> and recently performed comparative crystallographic studies on hPDPN in association with CLEC-2.<sup>(54)</sup> The interaction with CLEC-2 was mainly observed at Glu47 and Asp48 in the PLAG3 domain and the  $\alpha$ 2–6-linked sialic acid at Thr52 of hPDPN. Clone LpMab-12, our recently produced mAb, specifically detects this sialylated Thr52.<sup>(18)</sup>

Herein we used the CasMab technology for production of anti-hPDPN mAbs.<sup>(11)</sup> LN229/hPDPN cells were immunized into mice, and culture supernatants were screened using ELISA for binding to recombinant hPDPN, which was purified from LN229/hPDPN cells.<sup>(11)</sup> Finally, LpMab-19 (mouse IgG<sub>2b</sub>, kappa), the first IgG<sub>2b</sub> of mouse anti-hPDPN mAbs using CasMab technology, was produced after limiting dilution.

LpMab-19 reacted with LN229/hPDPN, and did not with LN229 (hPDPN-negative cell) in flow cytometry (Fig. 1A). LpMab-19 recognized endogenous hPDPN, which is expressed in LN319 (a glioblastoma cell line), whereas it did

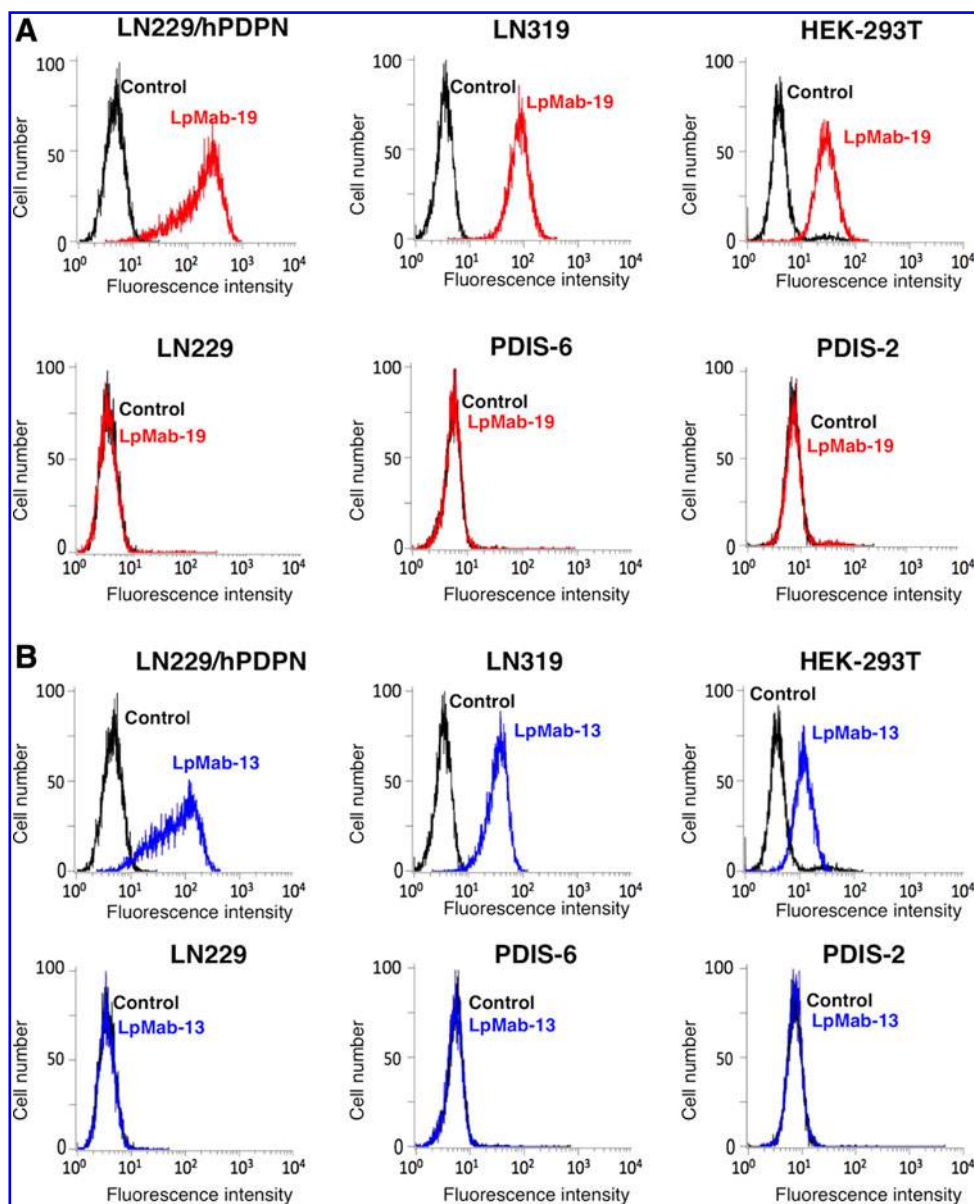


**FIG. 1.** In flow cytometry, LpMab-19 specifically detects hPDPN. (A) LN229, LN229/hPDPN, LN319, LN319/hPDPN-KO cell (PDIS-6), HEK-293T, and HEK-293T/hPDPN-KO cell (PDIS-2) were treated with LpMab-19 (1  $\mu$ g/mL; red) or control PBS (black) for 30 minutes at 4°C, followed by treatment with antimouse IgG-Oregon green. (B) LN229, LN229/hPDPN, LN319, LN319/hPDPN-KO cell (PDIS-6), HEK-293T, and HEK-293T/hPDPN-KO cell (PDIS-2) were treated with LpMab-13 (1  $\mu$ g/mL; blue) or control PBS (black) for 30 minutes at 4°C, followed by treatment with antimouse IgG-Oregon green. Fluorescence data were collected using a Cell Analyzer EC800. hPDPN, human podoplanin; PBS, phosphate-buffered saline.

not react with LN319/hPDPN-KO cell (PDIS-6) (Fig. 1A). In addition, LpMab-19 detected hPDPN of HEK-293T (an epithelial cell line of kidney), but lost the reaction with HEK-293T/hPDPN-KO cell (PDIS-2) (Fig. 1A). As a positive control, an anti-hPDPN mAb LpMab-13 was used (Fig. 1B).

LpMab-13 detected LN229/hPDPN, LN319, and HEK-293T, whereas it lost the reaction with PDIS-6 and PDIS-2.

We herein produced several deletion mutants of hPDPN, which were expressed in CHO-K1 cell lines. LpMab-19 detected the delta N-terminus (dN)23 that starts from Ala23.

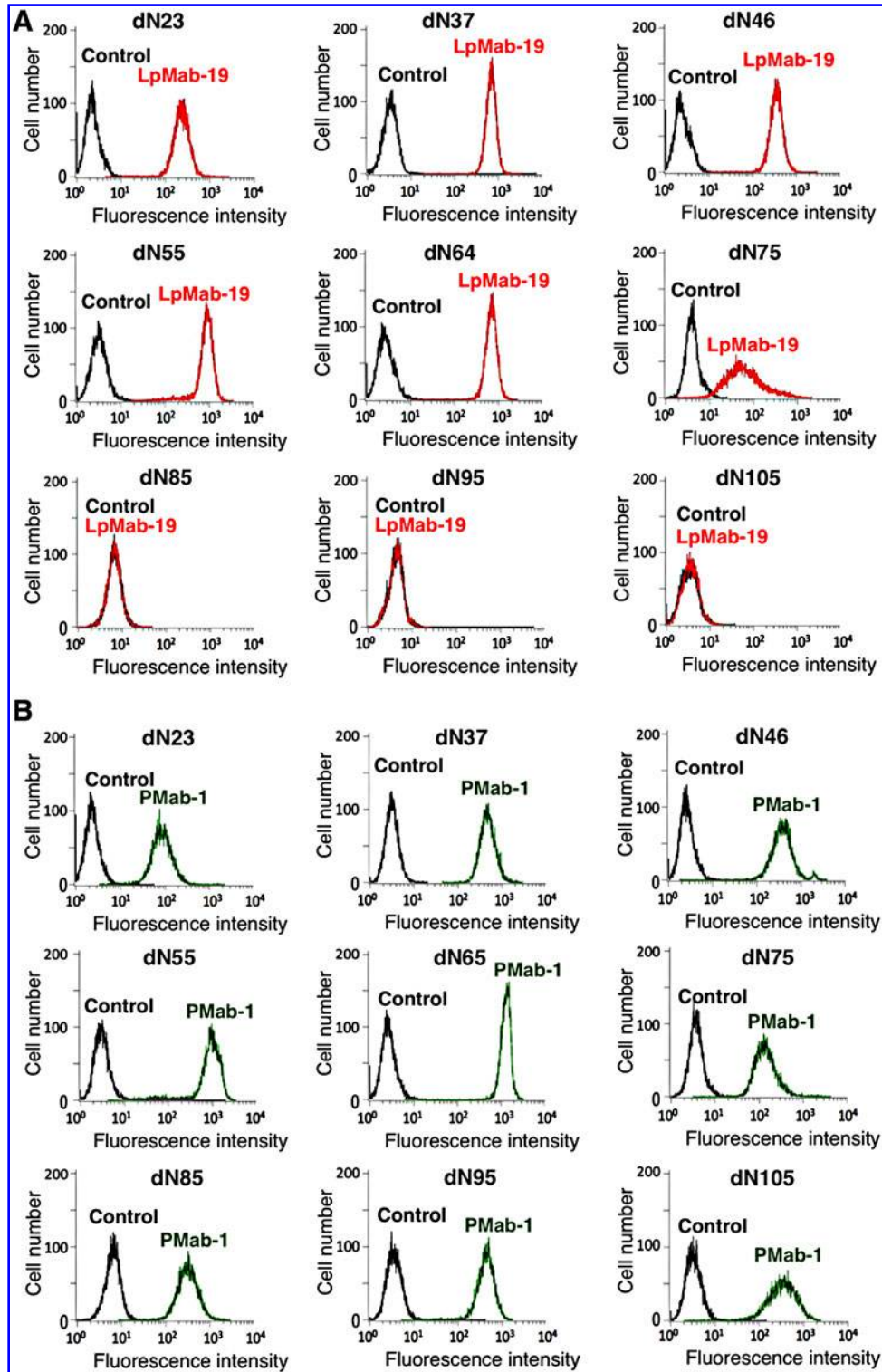


**FIG. 2.** Epitope mapping of LpMab-19 using deletion mutants of hPDPN in flow cytometry. Each hPDPN deletion mutant (dN23, dN37, dN46, dN55, dN64, dN75, dN85, dN95, and dN105) was treated with LpMab-19 (A, 1  $\mu$ g/mL; red), PMab-1 (anti-MAP tag; B, 1  $\mu$ g/mL; green), or control PBS (A, B; black) for 30 minutes at 4°C, followed by treatment with antimouse IgG or antirat IgG-Oregon green. Fluorescence data were collected using a Cell Analyzer EC800.

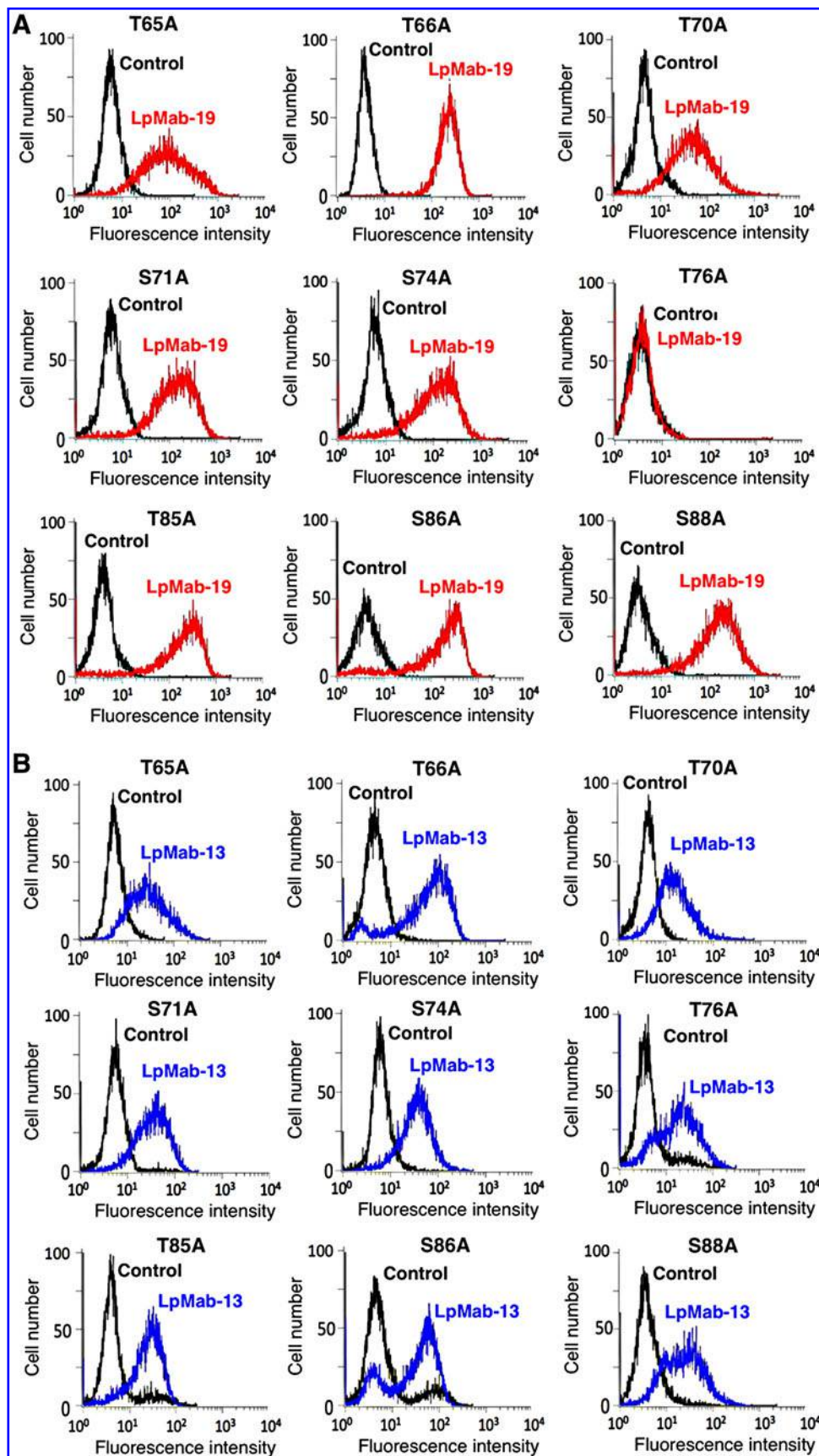


**FIG. 3.** Epitope mapping of LpMab-19 using point mutants of Ser/Thr residues of hPDPN in flow cytometry. Stable CHO-S transfectants expressing hPDPN point mutants (T65A, T66A, T70A, S71A, S74A, T76A, T85A, S86A, and S88A) were treated with LpMab-19 (A, 1  $\mu$ g/mL; red), LpMab-13 (B, 1  $\mu$ g/mL; blue), or control PBS (A, B; black) for 30 minutes at 4°C, followed by treatment with antimouse IgG-Oregon green. Fluorescence data were collected using a Cell Analyzer EC800. CHO, Chinese hamster ovary.

Similarly, LpMab-19 detected dN37, dN46, dN55, dN64, and dN75. In contrast, LpMab-19 lost the reaction with dN85, dN95, and dN105, indicating that the N-terminus of the LpMab-19 epitope exists between the 75th and 85th amino acids (Fig. 2A). All deletion mutants of hPDPN possess the N-terminal MAP tag and were detected by the anti-MAP tag mAb (clone: PMab-1) (Fig. 2B).

Next, we produced stable CHO-S cell lines expressing point mutants of hPDPN: T65A, T66A, T70A, S71A, S74A, T76A, T85A, S86A, and S88A (Fig. 3A). The epitope of LpMab-19 was thought to include glycans because LpMab-19 did not react with synthetic peptides of hPDPN (data not shown).

LpMab-19 lost the reaction with the T76A mutant, whereas the other point mutants were detected by LpMab-19 (Fig. 3A). All point mutants targeting Ser/Thr residues were detected by LpMab-13 (Fig. 3B). Therefore, the epitope of LpMab-19 includes sialic acid on *O*-glycan, which is attached to Thr76.

We further determined the LpMab-19 epitope using alanine scanning around Thr76 of hPDPN. Nine hPDPN point mutants against Ser74–Thr85 were transiently expressed in CHO-K1 cells. As shown in Figure 4A, LpMab-19 did not detect T76A, I78A, and R79A. In contrast, LpMab-13 recognized all point mutants (Fig. 4B), indicating that the minimum epitope of LpMab-19 was Thr76–Arg79.

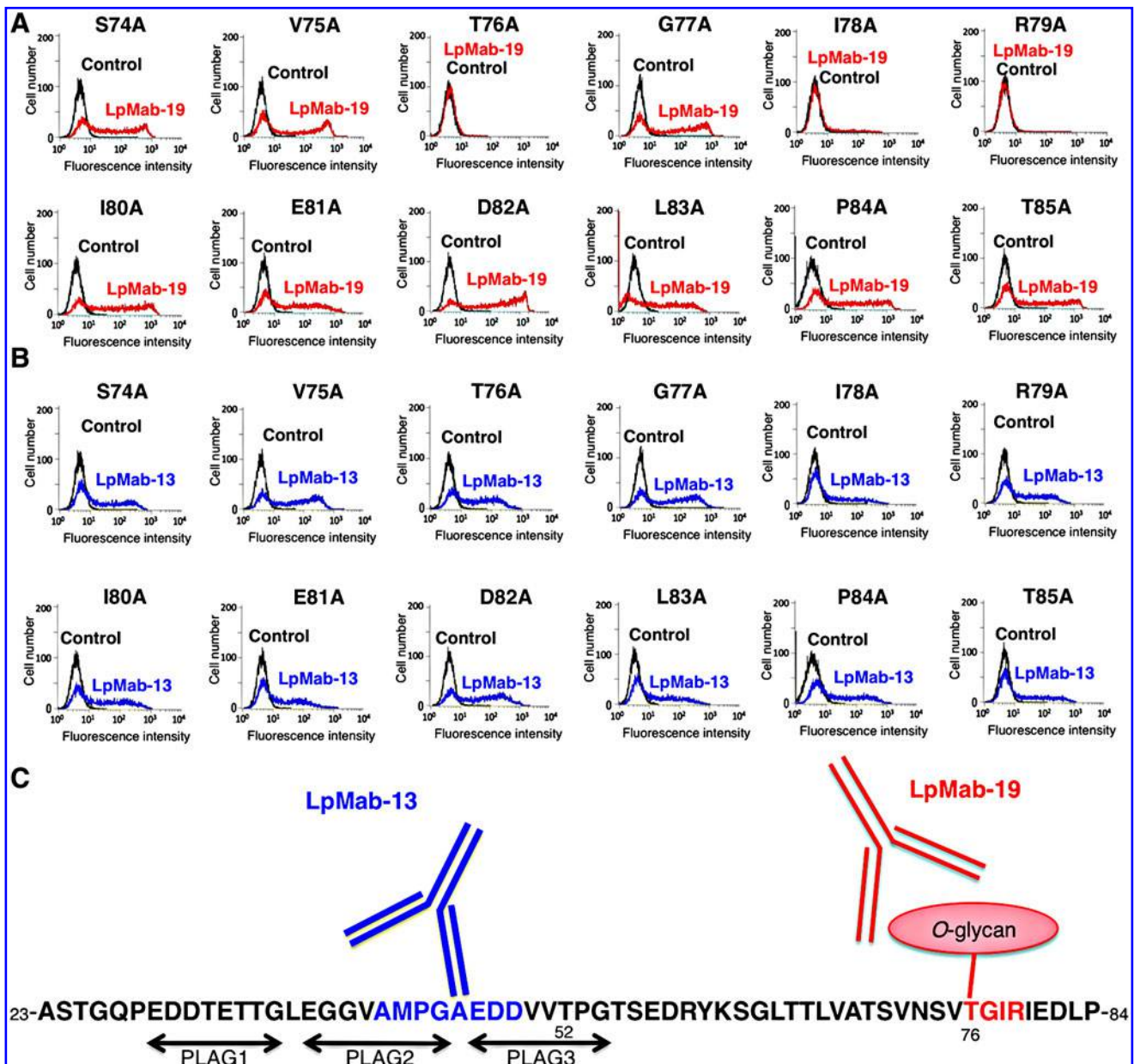


**FIG. 4.** Epitope mapping of LpMab-19 using point mutants of hPDPN in flow cytometry. Nine hPDPN point mutants against Ser74–Thr85 were transiently expressed in CHO-K1 cells. Cells were treated with LpMab-19 (A, 1  $\mu$ g/mL; red), LpMab-13 (B, 1  $\mu$ g/mL; blue), or control PBS (A, B; black) for 30 minutes at 4°C, followed by treatment with antimouse IgG-Oregon green. Fluorescence data were collected using a Cell Analyzer EC800. (C) Schematic illustration of the epitope of anti-hPDPN mAbs. mAbs, monoclonal antibodies.

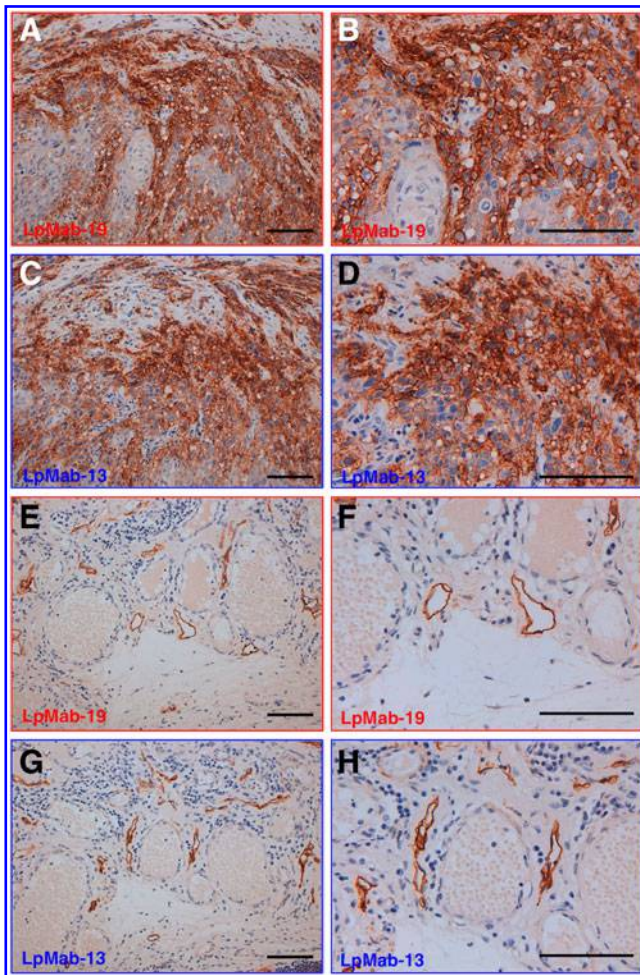


**FIG. 5.** Immunohistochemical analysis by LpMab-19 against oral squamous cell carcinoma. Sections were incubated with 1  $\mu\text{g}/\text{mL}$  of LpMab-19 (A, B, E, F) or LpMab-13 (C, D, G, H), followed by Envision+ kit, and color was developed using DAB and counterstained with hematoxylin. Scale bar: 100  $\mu\text{m}$ . DAB, 3,3-diaminobenzidine tetrahydrochloride.

It has been reported that hPDPN is expressed in many cancers, such as malignant brain tumor, mesothelioma, oral cancer, lung cancer, esophageal cancer, testicular tumor, and osteosarcoma.<sup>(13,38,44)</sup> Here we compared the reactivity of LpMab-19 and LpMab-13 in an immunohistochemical analysis using oral squamous cell carcinoma. LpMab-19 stained cancer cells (Fig. 5A, B) and LECs (Fig. 5E, F) in a membrane/cytoplasmic-staining pattern without an antigen retrieval procedure. LpMab-19 did not react with vascular endothelial cells (Fig. 5E, F). The staining pattern of LpMab-19 is similar to LpMab-13, indicating that LpMab-19 is very useful for immunohistochemistry.

Therefore, LpMab-19 could be useful for investigating the expression and function of hPDPN in cancers and normal tissues. In future, different epitope-possessing anti-hPDPN mAbs should be produced for uncovering the function of hPDPN.

#### Acknowledgments

We thank Takuro Nakamura, Noriko Saidoh, and Kanae Yoshida for their excellent technical assistance. We also

thank Yuki Fujii and Ryusuke Honma for their suggestion and advice. This work was supported, in part, by the Platform for Drug Discovery, Informatics, and Structural Life Science (PDIS) from Japan Agency for Medical Research and development, AMED (Y.K.), by the Regional Innovation Strategy Support Program from the Ministry of Education, Culture, Sports, Science and Technology (MEXT) of Japan (Y.K.), by JSPS KAKENHI Grant Number 26440019 (M.K.K.) and Grant Number 16K10748 (Y.K.), and by the Basic Science and Platform Technology Program for Innovative Biological Medicine from AMED (Y.K.). This work was performed, in part, under the Cooperative Research Program of Institute for Protein Research, Osaka University, CR-15-05 and CR-16-05 (Y.K.).

#### Author Disclosure Statement

No competing financial interests exist.

#### References

1. Tsuruo T, Kawabata H, Iida H, and Yamori T: Tumor-induced platelet aggregation and growth promoting factors as determinants for successful tumor metastasis. *Clin Exp Metastasis* 1986;4:25–33.
2. Sugimoto Y, Oh-hara T, Watanabe M, Saito H, Yamori T, and Tsuruo T: Acquisition of metastatic ability in hybridomas between two low metastatic clones of murine colon adenocarcinoma 26 defective in either platelet-aggregating activity or in vivo growth potential. *Cancer Res* 1987;47:4396–4401.
3. Watanabe M, Okochi E, Sugimoto Y, and Tsuruo T: Identification of a platelet-aggregating factor of murine colon adenocarcinoma 26: Mr 44,000 membrane protein as determined by monoclonal antibodies. *Cancer Res* 1988;48:6411–6416.
4. Watanabe M, Sugimoto Y, and Tsuruo T: Expression of a Mr 41,000 glycoprotein associated with thrombin-independent platelet aggregation in high metastatic variants of murine B16 melanoma. *Cancer Res* 1990;50:6657–6662.
5. Sugimoto Y, Watanabe M, Oh-hara T, Sato S, Isoe T, and Tsuruo T: Suppression of experimental lung colonization of a metastatic variant of murine colon adenocarcinoma 26 by a monoclonal antibody 8F11 inhibiting tumor cell-induced platelet aggregation. *Cancer Res* 1991;51:921–925.
6. Toyoshima M, Nakajima M, Yamori T, and Tsuruo T: Purification and characterization of the platelet-aggregating sialoglycoprotein gp44 expressed by highly metastatic variant cells of mouse colon adenocarcinoma 26. *Cancer Res* 1995;55:767–773.
7. Kato Y, Fujita N, Yano H, and Tsuruo T: Suppression of experimental lung colonization of mouse colon adenocarcinoma 26 in vivo by an anti-idiotypic monoclonal antibody recognizing a platelet surface molecule. *Cancer Res* 1997;57:3040–3045.
8. Kato Y, Fujita N, Kunita A, Sato S, Kaneko M, Osawa M, et al.: Molecular identification of Aggrus/T1alpha as a platelet aggregation-inducing factor expressed in colorectal tumors. *J Biol Chem* 2003;278:51599–51605.
9. Kunita A, Kashima TG, Morishita Y, Fukayama M, Kato Y, Tsuruo T, et al.: The platelet aggregation-inducing factor aggrus/podoplanin promotes pulmonary metastasis. *Am J Pathol* 2007;170:1337–1347.
10. Kaneko MK, Kato Y, Kitano T, and Osawa M: Conservation of a platelet activating domain of Aggrus/podoplanin

- as a platelet aggregation-inducing factor. *Gene* 2006;378:52–57.
11. Kato Y, and Kaneko MK: A cancer-specific monoclonal antibody recognizes the aberrantly glycosylated podoplanin. *Sci Rep* 2014;4:5924.
  12. Kaneko MK, Oki H, Hozumi Y, Liu X, Ogasawara S, Takagi M, et al.: Monoclonal antibody LpMab-9 recognizes O-glycosylated N-terminus of human podoplanin. *Monoclon Antib Immunodiagn Immunother* 2015;34:310–317.
  13. Kaneko MK, Oki H, Ogasawara S, Takagi M, and Kato Y: Anti-podoplanin monoclonal antibody LpMab-7 detects metastatic lesions of osteosarcoma. *Monoclon Antib Immunodiagn Immunother* 2015;34:154–161.
  14. Kato Y, Kunita A, Abe S, Ogasawara S, Fujii Y, Oki H, et al.: The chimeric antibody chLpMab-7 targeting human podoplanin suppresses pulmonary metastasis via ADCC and CDC rather than via its neutralizing activity. *Oncotarget* 2015;6:36003–36018.
  15. Ogasawara S, Oki H, Kaneko MK, Hozumi Y, Liu X, Honma R, et al.: Development of monoclonal antibody LpMab-10 recognizing non-glycosylated PLAG1/2 domain including Thr34 of human podoplanin. *Monoclon Antib Immunodiagn Immunother* 2015;34:318–326.
  16. Oki H, Kaneko MK, Ogasawara S, Tsujimoto Y, Liu X, Sugawara M, et al.: Characterization of a monoclonal antibody LpMab-7 recognizing non-PLAG domain of podoplanin. *Monoclon Antib Immunodiagn Immunother* 2015;34:174–180.
  17. Oki H, Ogasawara S, Kaneko MK, Takagi M, Yamauchi M, and Kato Y: Characterization of monoclonal antibody LpMab-3 recognizing sialylated glycopeptide of podoplanin. *Monoclon Antib Immunodiagn Immunother* 2015;34:44–50.
  18. Kato Y, Ogasawara S, Oki H, Goichberg P, Honma R, Fujii Y, et al.: LpMab-12 established by CasMab technology specifically detects sialylated O-glycan on Thr52 of platelet aggregation-stimulating domain of human podoplanin. *PLoS One* 2016;11:e0152912.
  19. Kato Y, Ogasawara S, Oki H, Honma R, Takagi M, Fujii Y, et al.: Novel monoclonal antibody LpMab-17 developed by CasMab technology distinguishes human podoplanin from monkey podoplanin. *Monoclon Antib Immunodiagn Immunother* 2016;35:109–116.
  20. Ogasawara S, Kaneko MK, Honma R, Oki H, Fujii Y, Takagi M, et al.: Establishment of mouse monoclonal antibody LpMab-13 against human podoplanin. *Monoclon Antib Immunodiagn Immunother* 2016;35:155–162.
  21. Kato Y, Kaneko MK, Kuno A, Uchiyama N, Amano K, Chiba Y, et al.: Inhibition of tumor cell-induced platelet aggregation using a novel anti-podoplanin antibody reacting with its platelet-aggregation-stimulating domain. *Biochem Biophys Res Commun* 2006;349:1301–1307.
  22. Ogasawara S, Kaneko MK, Price JE, and Kato Y: Characterization of anti-podoplanin monoclonal antibodies: Critical epitopes for neutralizing the interaction between podoplanin and CLEC-2. *Hybridoma* 2008;27:259–267.
  23. Kato Y, Vaidyanathan G, Kaneko MK, Mishima K, Srivastava N, Chandramohan V, et al.: Evaluation of anti-podoplanin rat monoclonal antibody NZ-1 for targeting malignant gliomas. *Nucl Med Biol* 2010;37:785–794.
  24. Fujii Y, Kaneko M, Neyazaki M, Nogi T, Kato Y, and Takagi J: PA tag: A versatile protein tagging system using a super high affinity antibody against a dodecapeptide derived from human podoplanin. *Protein Expr Purif* 2014;95:240–247.
  25. Fujii Y, Matsunaga Y, Arimori T, Kitago Y, Ogasawara S, Kaneko MK, et al.: Tailored placement of a turn-forming PA tag into the structured domain of a protein to probe its conformational state. *J Cell Sci* 2016;129:1512–1522.
  26. Chandramohan V, Bao X, Kato Kaneko M, Kato Y, Keir ST, Szafranski SE, et al.: Recombinant anti-podoplanin (NZ-1) immunotoxin for the treatment of malignant brain tumors. *Int J Cancer* 2013;132:2339–2348.
  27. Kaneko MK, Kunita A, Abe S, Tsujimoto Y, Fukayama M, Goto K, et al.: Chimeric anti-podoplanin antibody suppresses tumor metastasis through neutralization and antibody-dependent cellular cytotoxicity. *Cancer Sci* 2012;103:1913–1919.
  28. Kato Y, Kaneko MK, Kunita A, Ito H, Kameyama A, Ogasawara S, et al.: Molecular analysis of the pathophysiological binding of the platelet aggregation-inducing factor podoplanin to the C-type lectin-like receptor CLEC-2. *Cancer Sci* 2008;99:54–61.
  29. Abdelmoula M, Spertini F, Shibata T, Gyotoku Y, Luzuy S, Lambert PH, et al.: IgG3 is the major source of cryoglobulins in mice. *J Immunol* 1989;143:526–532.
  30. Takagi S, Sato S, Oh-hara T, Takami M, Koike S, Mishima Y, et al.: Platelets promote tumor growth and metastasis via direct interaction between Aggrus/podoplanin and CLEC-2. *PLoS One* 2013;8:e73609.
  31. Nakazawa Y, Takagi S, Sato S, Oh-hara T, Koike S, Takami M, et al.: Prevention of hematogenous metastasis by neutralizing mice and its chimeric anti-Aggrus/podoplanin antibodies. *Cancer Sci* 2011;102:2051–2057.
  32. Marks A, Sutherland DR, Bailey D, Iglesias J, Law J, Lei M, et al.: Characterization and distribution of an oncofetal antigen (M2A antigen) expressed on testicular germ cell tumours. *Br J Cancer* 1999;80:569–578.
  33. Kono T, Shimoda M, Takahashi M, Matsumoto K, Yoshimoto T, Mizutani M, et al.: Immunohistochemical detection of the lymphatic marker podoplanin in diverse types of human cancer cells using a novel antibody. *Int J Oncol* 2007;31:501–508.
  34. Sekiguchi T, Takemoto A, Takagi S, Takatori K, Sato S, Takami M, et al.: Targeting a novel domain in podoplanin for inhibiting platelet-mediated tumor metastasis. *Oncotarget* 2016;7:3934–3946.
  35. Hayatsu N, Ogasawara S, Kaneko MK, Kato Y, and Narimatsu H: Expression of highly sulfated keratan sulfate synthesized in human glioblastoma cells. *Biochem Biophys Res Commun* 2008;368:217–222.
  36. Kaji C, Tsujimoto Y, Kato Kaneko M, Kato Y, and Sawa Y: Immunohistochemical examination of novel rat monoclonal antibodies against mouse and human podoplanin. *Acta Histochem Cytochem* 2012;45:227–237.
  37. Honma R, Ogasawara S, Kaneko M, Fujii Y, Oki H, Nakamura T, et al.: PMab-44 detects bovine podoplanin in immunohistochemistry. *Monoclon Antib Immunodiagn Immunother* 2016. DOI:10.1089/mab.2016.0016.
  38. Martin-Villar E, Scholl FG, Gamallo C, Yurrita MM, Munoz-Guerra M, Cruces J, et al.: Characterization of human PA2.26 antigen (T1alpha-2, podoplanin), a small membrane mucin induced in oral squamous cell carcinomas. *Int J Cancer* 2005;113:899–910.
  39. Yuan P, Temam S, El-Naggar A, Zhou X, Liu D, Lee J, et al.: Overexpression of podoplanin in oral cancer and its association with poor clinical outcome. *Cancer* 2006;107:563–569.

40. Takagi S, Oh-Hara T, Sato S, Gong B, Takami M, and Fujita N: Expression of Aggrus/podoplanin in bladder cancer and its role in pulmonary metastasis. *Int J Cancer* 2014;134:2605–2614.
41. Kunita A, Kashima TG, Ohazama A, Grigoriadis AE, and Fukayama M: Podoplanin is regulated by AP-1 and promotes platelet aggregation and cell migration in osteosarcoma. *Am J Pathol* 2011;179:1041–1049.
42. Mishima K, Kato Y, Kaneko MK, Nakazawa Y, Kunita A, Fujita N, et al.: Podoplanin expression in primary central nervous system germ cell tumors: A useful histological marker for the diagnosis of germinoma. *Acta Neuropathol (Berl)* 2006;111:563–568.
43. Mishima K, Kato Y, Kaneko MK, Nishikawa R, Hirose T, and Matsutani M: Increased expression of podoplanin in malignant astrocytic tumors as a novel molecular marker of malignant progression. *Acta Neuropathol (Berl)* 2006;111:483–488.
44. Abe S, Morita Y, Kaneko MK, Hanibuchi M, Tsujimoto Y, Goto H, et al.: A novel targeting therapy of malignant mesothelioma using anti-podoplanin antibody. *J Immunol* 2013;190:6239–6249.
45. Kato Y, Sasagawa I, Kaneko M, Osawa M, Fujita N, and Tsuruo T: Aggrus: A diagnostic marker that distinguishes seminoma from embryonal carcinoma in testicular germ cell tumors. *Oncogene* 2004;23:8552–8556.
46. Kato Y, Kaneko M, Sata M, Fujita N, Tsuruo T, and Osawa M: Enhanced expression of Aggrus (T1alpha/podoplanin), a platelet-aggregation-inducing factor in lung squamous cell carcinoma. *Tumor Biol* 2005;26:195–200.
47. Pula B, Jethon A, Piotrowska A, Gomulkiewicz A, Owczarek T, Calik J, et al.: Podoplanin expression by cancer-associated fibroblasts predicts poor outcome in invasive ductal breast carcinoma. *Histopathology* 2011;59:1249–1260.
48. Kawase A, Ishii G, Nagai K, Ito T, Nagano T, Murata Y, et al.: Podoplanin expression by cancer associated fibroblasts predicts poor prognosis of lung adenocarcinoma. *Int J Cancer* 2008;123:1053–1059.
49. Hoshino A, Ishii G, Ito T, Aoyagi K, Ohtaki Y, Nagai K, et al.: Podoplanin-positive fibroblasts enhance lung adenocarcinoma tumor formation: Podoplanin in fibroblast functions for tumor progression. *Cancer Res* 2011;71:4769–4779.
50. Schoppmann SF, Jesch B, Riegler MF, Maroske F, Schwameis K, Jomrich G, et al.: Podoplanin expressing cancer associated fibroblasts are associated with unfavourable prognosis in adenocarcinoma of the esophagus. *Clin Exp Metastasis* 2013;30:441–446.
51. Shindo K, Aishima S, Ohuchida K, Fujiwara K, Fujino M, Mizuuchi Y, et al.: Podoplanin expression in cancer-associated fibroblasts enhances tumor progression of invasive ductal carcinoma of the pancreas. *Mol Cancer* 2013;12:168.
52. Inoue H, Tsuchiya H, Miyazaki Y, Kikuchi K, Ide F, Sakashita H, et al.: Podoplanin expressing cancer-associated fibroblasts in oral cancer. *Tumour Biol* 2014;35:11345–11352.
53. Suzuki-Inoue K, Kato Y, Inoue O, Kaneko MK, Mishima K, Yatomi Y, et al.: Involvement of the snake toxin receptor CLEC-2, in podoplanin-mediated platelet activation, by cancer cells. *J Biol Chem* 2007;282:25993–26001.
54. Nagae M, Morita-Matsumoto K, Kato M, Kaneko MK, Kato Y, and Yamaguchi Y: A platform of C-type lectin-like receptor CLEC-2 for binding O-glycosylated podoplanin and nonglycosylated rhodocytin. *Structure* 2014;22:1711–1721.

Address correspondence to:

*Dr. Yukinari Kato*

*Department of Regional Innovation*

*Tohoku University Graduate School of Medicine*

*2-1 Seiryomachi, Aoba-ku*

*Sendai*

*Miyagi 980-8575*

*Japan*

*E-mail: yukinari-k@bea.hi-ho.ne.jp;  
yukinarikato@med.tohoku.ac.jp*

*Received: June 18, 2016*

*Accepted: August 1, 2016*